

## RESEARCH ARTICLE

# Green Logistics Tram Charging and Path Optimization Considering Urban Impedance

LEI FU<sup>1</sup>, YAN XU<sup>1</sup>, AND AOBEI ZHANG<sup>2</sup><sup>1</sup>School of Science and Technology, Shenyang Polytechnic College, Shenyang 110045, China<sup>2</sup>School of Management, Shenyang University of Technology, Shenyang 100870, China

Corresponding author: Lei Fu (mark\_2023@163.com)

This work was supported in part by the Research on the Effective Connection Mechanism Between Middle and High Schools in the Digital Innovation Ecosystem under Project JG22EA008; and in part by the Ministry of Education, Centre for Scientific Research and Development of Colleges and Universities, Special Project “Innovative Application of Virtual Simulation Technology in Vocational Education Teaching,” under Project ZJXF2022012.

**ABSTRACT** The aim of this article is to investigate the optimization of electric vehicle charging and swapping for green logistics, as well as path planning considering urban impedance. We improved a road impedance function model suitable for urban road traffic in China to calculate the actual traffic time based on real-time traffic data and the intricate urban road environment. This model is then applied to address the delivery optimization problem. Furthermore, a robust computational approach is introduced to estimate battery degradation costs, accounting for environmental temperature and depth of discharge. The logistics delivery model is effectively tackled using genetic algorithms, and simulation results demonstrate the considerable advantages of electric vehicle swapping, effectively mitigating energy wastage and environmental pollution. Additionally, the integration of road impedance modeling for path optimization proves to significantly reduce logistics costs, time expenditures, and enhance logistics efficiency. A comprehensive sensitivity analysis is also conducted to elucidate the factors influencing electric vehicle battery degradation, revealing a direct correlation between higher temperatures, deeper discharge depth, and increased battery loss. The study underscores the paramount significance of this research for the development and optimization of urban green logistics systems.

**INDEX TERMS** Green logistics, road impedance function, electric vehicle, genetic algorithms, battery degradation costs.

## I. INTRODUCTION

As urbanization advances, the quandary of urban logistics has garnered escalating attention. The burgeoning urban populace has engendered a substantial demand for goods and commodities, precipitating a marked upsurge in the magnitude of logistics transportation. This surge has not only exerted immense strain on road traffic but has also compounded the predicaments of urban traffic congestion and environmental degradation. Ineffective traffic organization and planning within urban environs have engendered inefficiency and escalated expenses in logistics and distribution [1]. The pervasive deployment of conventional fuel-powered vehicles in urban

logistics has engendered environmental quandaries, encompassing air and noise pollution, substantially impacting the well-being and standard of living of urban denizens [2]. Consequently, the urban logistics predicament not only curtails the advancement of urban economies but also impinges upon the residents' quality of life and the sustainable development of the environment. In light of such circumstances, the quest for an environmentally sustainable and efficacious urban logistics remedy has become imperative.

Sustainable logistics represents an inexorable trend in contemporary societal progress, and electric vehicles, as pivotal agents of sustainable logistics, underscore the profound import of optimizing their vehicle charging and swapping routes. Primarily, the optimization of charging and swapping routes can augment the transportation efficiency of

The associate editor coordinating the review of this manuscript and approving it for publication was Junho Hong<sup>1</sup>.

electric vehicles. Through judiciously delineating the spatial arrangement of charging and swapping stations, the charging and swapping duration of electric vehicles can be curtailed, thereby mitigating disruptions and lateness in logistics distribution and enhancing the efficiency and timeliness of logistics transportation. This holds momentous implications for catering to the surging logistics requisites in urban locales while attenuating traffic congestion and environmental degradation [3]. Secondly, optimizing vehicle charging and swapping routes can yield environmental and societal dividends. The prevalence of electric vehicles can abate tailpipe emissions and noise pollution, ameliorating urban air quality and residents' living milieu. Strategic placement of charging and power exchange stations can avert encroachment on residents' daily lives, abate urban congestion and vehicular mishaps, and elevate urban residents' quality of life. Furthermore, optimizing vehicle charging and swapping routes can galvanize the electric vehicle industry. By judiciously orchestrating the establishment of charging and power exchange stations, a more expedient and dependable infrastructure can be furnished for the propagation and advancement of electric vehicles [4], fostering the robust evolution of the electric vehicle industry, fostering the flourishing progression of allied industries, and injecting fresh vitality into the sustainable advancement of urban economies.

The concept of road impedance delineates the resistance that vehicles encounter while traversing roads, bearing substantial significance in the realm of logistics transport. By accounting for road impedance, the optimal planning of goods transport paths can be orchestrated, thereby enhancing transport efficiency and curbing transport expenses. In contemporary logistics management, the employment of road impedance theory facilitates a more precise evaluation of the challenges posed by diverse roads, enabling the selection of the most favorable transport routes, averting congestion and vehicular accidents, and elevating the punctuality and security of goods delivery [5]. Furthermore, the consideration of road impedance can also galvanize the advancement of sustainable logistics, as exemplified by the reduction of vehicle mileage, thereby lessening environmental impact and effectuating the greening of logistics transport [6]. Hence, in the domain of logistics transport, judicious contemplation of road impedance not only augments transport efficiency and cost-effectiveness but also propels the logistics industry towards a more sustainable and ecofriendly trajectory.

In summary, the incorporation of the urban road impedance function in logistics and transport not only enhances the precision and applicability of path planning but also streamlines vehicle routes, curtails expenses, and fortifies the adaptability and flexibility of the system. Particularly in championing green logistics and sustainable innovation, the employment of the urban road impedance function is profoundly consequential. Through optimizing path planning and reducing vehicular mileage, it is feasible to diminish energy consumption and carbon emissions, thereby fostering the advancement of green logistics in alignment with the exigency for

sustainable development in contemporary society. Additionally, amalgamating green innovation principles and the urban road impedance function with intelligent traffic signals, electric vehicle charging stations, and other urban intelligent infrastructure augments the efficiency of logistics and distribution, diminishes environmental impact, and actualizes the eco-friendly transformation in the realm of logistics. Hence, bolstering the research and integration of the urban road impedance function in logistics and transport not only meets the requisites of urban logistics development but also propels the comprehensive realization of green logistics and sustainable innovation.

## II. RELATED WORK

In this section, the relevant research on green logistics tram charging and swapping and path optimization considering urban impedance was discussed.

### A. ROAD TRAFFIC

Urban road impedance encompasses the hindrances to urban traffic traversal arising from factors such as traffic flow, intersections, speed limits, and other elements, exerting a substantial influence on logistics transport. Research indicates that the inclusion of urban road impedance can enable logistics enterprises to enhance distribution path planning and elevate transport efficiency. Within urban settings, the intricate nature of road impedance and traffic congestion poses myriad challenges to logistics and distribution. In response to these challenges, scholars have scrutinized the factors influencing road impedance in diverse urban locales, probing the effects of traffic congestion, intersection density, and speed limit demarcations. For instance, Wang et al. [7] employed discrete-time Markov chains and real-time traffic monitoring data to prognosticate the likelihood of traffic congestion and discern the ramifications of highway traffic on distribution. Xu et al. [8], on the other hand, leveraged the Davidson road impedance function to compute transport durations. Furthermore, Zhang [9] proposed a method for managing congested roadways based on traffic allocation to address urban traffic congestion. Younes and Boukerche [10] devised a dynamic and efficient traffic signal scheduling algorithm that adjusts optimal green phase durations for each traffic flow based on real-time traffic conditions around signalized intersections. Additionally, Chen et al. [11] explored the impact of traffic congestion on cold-chain logistics in former warehouses and quantified congestion levels employing the congestion index. Some researchers have undertaken comparative evaluations of distinct road impedance models to ascertain which is best suited for enhancing transport efficiency and reducing costs within urban logistics and distribution models. Guo [12] formulated a time-dependent model for the green vehicle path problem with time windows in cold chain logistics, accounting for the time-dependent influence of traffic congestion. Similarly, Zhao [13] designed an electric vehicle path problem model under time-varying traffic conditions for

urban cold chain logistics planning, predicated on real-time traffic intelligence and the intricate urban road milieu. Lastly, Zhang [14] developed a mathematical model for optimizing cold chain logistics and distribution paths, considering the impact of road impedance.

## B. GREEN LOGISTICS

Green logistics encompasses the adoption of environmentally sustainable, energy-efficient, and low-carbon methodologies in the transportation and distribution processes within logistics, aimed at mitigating environmental impact. This encompasses strategies such as the integration of clean energy sources, optimization of transport routes, and reduction of packaging waste to foster eco-friendly logistics operations. The evolution of green logistics has emerged as a significant trend within the global logistics industry, not only alleviating environmental burdens but also enhancing corporate reputation and competitiveness. Electric vehicle (EV) transportation, as a facet of green logistics, has garnered substantial attention. As electric vehicle technology continues to advance and governmental backing for clean energy vehicles grows, the deployment of electric vehicles in logistics transportation is on the rise. Electric vehicles offer the advantages of zero emissions, low noise, and energy conservation, thereby significantly contributing to the amelioration of urban air quality and the reduction of noise pollution. Nonetheless, electric vehicle transportation encounters challenges relating to charging infrastructure development, range limitations, and cost management [15]. Presently, research on EVs encompassing charging infrastructure, EV adoption, thermal management systems, and routing issues has emerged as a prominent thematic focus in recent years [16]. For instance, Li [17] constructed an analytical model to examine the influence of EV anxiety and the environmental advantages of EVs on optimal subsidy and pricing determinations. Imre [18] conducted a study on the factors influencing the preference for EV utilization, seeking to estimate their prospective adoption rate in urban freight transport. Additionally, Timilsina [19] meticulously explained the mechanisms leading to battery degradation within electric vehicles, delving into the primary factors contributing to degradation during vehicle operations and their implications for batteries. With burgeoning environmental consciousness and incentivization from governmental policies, electric vehicles (EVs) are increasingly being integrated into logistics and distribution operations. Considering green power trading and carbon emissions, Qiang [20] addressed the green vehicle routing problem (GVRP) and devised an EV routing model with time windows to minimize overall costs. Moreover, Zhou [21] formulated an EV routing problem (EVRP-BS-MTW) accounting for battery replacement and hybrid time window constraints. Shangguan [22] proposed EV battery charging planning by factoring in the cost of charging facilities for logistics vehicles and fuel consumption expenses.

## C. SOLUTION METHOD

As planning models evolve and the scale of nodes expands, traditional intelligent optimization algorithms exhibit certain limitations in addressing vehicle routing problems (VRP). Consequently, numerous scholars have delved into profound investigations of intelligent optimization algorithms. Many enhanced and hybrid optimization algorithms have been devised to tackle the objective model. For instance, Zhao et al. [23] delved into a multi-objective path optimization model centered on cost, carbon emissions, and customer satisfaction, devising an improved ant colony algorithm solution model utilizing a multi-objective heuristic function. Zhang et al. [24] crafted an optimization algorithm amalgamating RNA computation and an ant colony algorithm to surmount VRPs. Qin et al. [25] formulated a cold-chain path optimization model focusing on minimizing customer satisfaction costs, proposing a circular evolutionary genetic algorithm to compute the model. Ren et al. [26] formulated a multi-distribution-center cold-chain logistics path optimization model considering soft time window constraints, employing a hybrid algorithm of artificial fish swarms and ant colonies to solve the model. Song et al. [27] devised a specialized coding method to enhance the artificial fish swarming algorithm by considering the distinct characteristics of various vehicle models. Zhu and Hu [28] established a cold-chain logistics path optimization model minimizing total cost while factoring in fuel consumption and traffic congestion. A hybrid genetic-ant colony algorithm based on response surface methodology was proposed to tackle the model. Wang and Wen [29] presented an adaptive genetic algorithm to address the low-carbon cold-chain logistics distribution path problem. Moreover, Chen et al. [30] scrutinized the robust global search capability of the improved ant colony algorithm and the favorable local search capability of the forbidden search algorithm, leading to the development of a hybrid optimization algorithm to resolve VRP.

In summary, in the realm of logistics and transportation, research has predominantly centered on exploring the influence of traffic congestion, speed, and real-time road conditions on vehicle path optimization. However, the consideration of road impedance in electric vehicle (EV) transport studies has been scant. Road impedance directly impacts actual transport time and indirectly influences the cost per delivery in vehicle transport. Consequently, the assessment of the impact of road impedance on green logistics transport assumes paramount significance. Furthermore, within the domain of green logistics, the investigation of electric vehicle distribution and the intricacies of charging and switching methods remains pertinent. Thus, this study aims to address the lacuna by proposing a model for electric vehicle logistics path optimization, taking into account road impedance, and aiming to minimize the total cost while considering charging and switching modes. Additionally, a genetic algorithm

is devised to tackle this Electric Vehicle Routing Problem (EVRP) model.

### III. ROAD IMPEDANCE FUNCTION ANALYSIS AND IMPROVEMENT

The Bureau of Public Roads (BPR) function is the traditional model for calculating the impedance function of a road section. The traditional BRP function serves as a conventional model for computing the impedance function of a road section. However, it exhibits certain limitations. Firstly, it fails to depict the actual scenario of road impedance when the traffic volume exceeds the capacity of the road section. Furthermore, for road sections with low traffic volumes, a higher parameter value leads to temporal impedance approaching the free-flow time in an infinitely close manner. The expression is

$$t = t_0 \left( 1 + \alpha \left( \frac{Q}{C} \right)^\beta \right) \quad (1)$$

where  $t_0$  is the free passage time during zero flow on the road segment,  $Q$  is the traffic volume on the road segment,  $C$  is the traffic capacity on the road segment, and  $\alpha$  and  $\beta$  are parameters to be calibrated. The values recommended by the U.S. Highway Department are  $\alpha = 0.15$  and  $\beta = 4.0$ .

The urban road impedance function consists of two parts: roadway impedance and intersection impedance. The actual travel time of urban road impedance is given by

$$T = T_1 + T_2 \quad (2)$$

where  $T_1$  is the travel time of roadway impedance and  $T_2$  is the travel time of intersection impedance.

To address the deficiencies of the BPR function and ensure that traffic flow is not constrained by traffic capacity, we adopt Wang's [31] concept to enhance the BPR function.

By elucidating the interplay among the three urban-road parameters (velocity, density, and traffic volume), one can derive the relationship between density and traffic volume. This relationship can be expressed linearly as follows:

$$Q = VK \quad (3)$$

The linear relationship between velocity  $V$  and density in the Greenshield model can be expressed as

$$V = V_f \left( 1 - \frac{K}{K_j} \right) \quad (4)$$

where  $V_f$  is the speed of free travel,  $K$  is the traffic density, and  $K_j$  is the density of road blockage at a vehicle speed of zero.

Substituting Eq. (4) into Eq. (3) yields

$$Q = V_f K - \frac{V_f}{K_j} K^2 \quad (5)$$

Let  $dQ/dK = 0$ . Then, when  $V = 0.5V_f$ ,  $K = 0.5K_j$ ,  $Q$  has a maximum value of  $0.25V_f K_j$ . The traffic volume at this point is the traffic capacity of the roadway. that is  $C = 0.25V_f K_j$ .

Substituting Eqs. (5) and  $C = 0.25V_f K_j$  into Eq. (1) yields

$$t = t_0 \left( 1 + \alpha \left( 1 - \left( 1 - \frac{K}{K_j} \right)^2 \right)^\beta \right) \quad (6)$$

$$K \in [0, 2K_j]$$

From the above, the degree of saturation  $Q/C$  is replaced by the density formula. Letting  $x = Q/C$ , we have

$$x = 1 - \left( 1 - \frac{K}{K_j} \right)^2 \quad (7)$$

We used the road impedance function model proposed by SPIESS [32]:

$$T_1 = t_0 \left( 2 + \sqrt{\beta^2 (1-x)^2 + \gamma^2} - \beta(1-x) - \gamma \right) \quad (8)$$

where  $\gamma = \frac{2\beta-1}{2\beta-2}$ ,  $\alpha > 0$ ,  $\beta > 1$ , and the degree of saturation is  $x = 1 - (1 - K/K_j)^2$ .

In China's urban road intersections, which have different forms, to facilitate the calculation, we assumed that the signal intersection for a type. Among them, the Webster model is a well-known model for calculating road signal intersection delays [33]:

$$T_2 = \frac{c(1-\lambda)^2}{2(1-\lambda x)} + \frac{x^2}{2Q(1-x)} - 0.65 \left( \frac{c}{Q^2} \right)^{\frac{1}{3}} x^{(2+5x)} \quad (9)$$

where  $Z_2$  is the time impedance of vehicles (i.e., vehicle delays),  $c$  is the signal cycle,  $x$  is the saturation level of the road,  $\lambda$  is the ratio of green lights to signal lights, and  $Q$  is the traffic flow arriving at the intersection. The first part of this equation is the basic delay term resulting from vehicles arriving at the intersection and stopping or queuing. The second part is the random delay term. The third part is the correction term for the random delay term. Webster's later study revealed that the third component was less weighted in the overall model. Therefore, the equation can be simplified as

$$T_2 = \frac{9}{10} \left[ \frac{c(1-\lambda)^2}{2(1-\lambda x)} + \frac{x^2}{2Q(1-x)} \right] \quad (10)$$

Therefore, the urban road impedance function is a function of the traffic density  $K$ :

$$\begin{aligned} T &= T_1 + T_2 \\ &= t_0 \left( 2 + \sqrt{\beta^2 (1-x)^2 + \gamma^2} - \beta(1-x) - \gamma \right) \\ &\quad + \frac{9}{10} \left[ \frac{c(1-\lambda)^2}{2(1-\lambda x)} + \frac{x^2}{2Q(1-x)} \right] \end{aligned} \quad (11)$$

where  $x = 1 - (1 - K/K_j)^2$ ,  $\gamma = 2\beta - 1/2\beta - 2$ , and  $\alpha$  and  $\beta$  are parameters to be calibrated. In this study, we used the U.S. Highway Department recommended values of  $\alpha = 0.15$  and  $\beta = 4.0$ .



**A. DATA COLLECTION**

The section between the subway entrance of Central Street and the Shenyang University of Technology in the Tiexi District, Shenyang, was selected for an example analysis. The data acquisition methods commonly used were the photographic method and the access method. Because the survey road section is not obscured by shelters, the photographic method was used to obtain relevant data such as road traffic density.

We collected traffic data from 06:00 to 21:00 on this road section. In Figs. 1 and 2, the curves represent the trends in traffic density and saturation from 06:00 to 11:00 and from 17:00 to 21:00, respectively. The trends of traffic density and saturation from 6:00 to 11:00 and from 17:00 to 21:00 show that the traffic density varies with saturation.

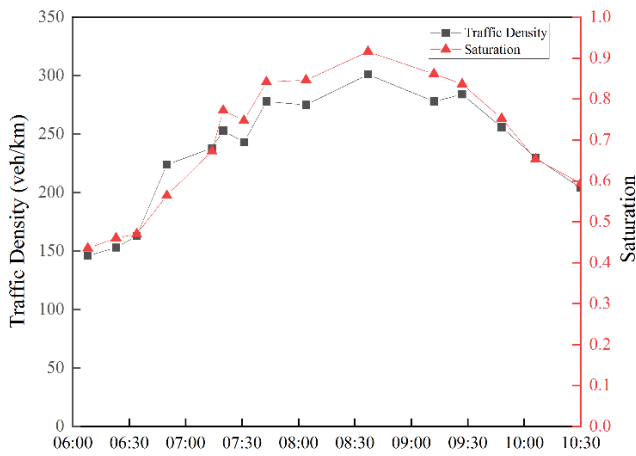


**FIGURE 1.** Change of saturation and traffic density.

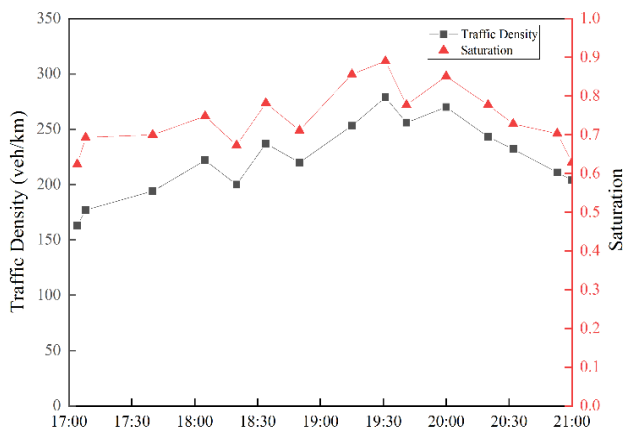


**FIGURE 2.** Change of saturation and traffic density.

**B. MODEL COMPARISON AND VALIDATION**

Roadway data collected at 18:00 were taken as an example. We obtained the traffic density of each road section  $K$ , and intersection traffic volumes  $Q$  using a road blockage density

of  $K_j = 125$ vehicles/km and parameters  $\alpha = 0.15$  and  $\beta = 4.0$ .

Utilizing the BPR road impedance function model, the enhanced road impedance function equation proposed by Wang [31], and the novel road impedance function model developed in this study, we computed the travel time along the road section from 06:00 to 21:00. Subsequently, the results obtained from these three road impedance functions were compared and validated against the actual driving time. The comparative analysis revealed that the total travel time estimated using the BPR function notably underestimates the actual values. This discrepancy can be attributed to the inherent limitation of the BPR road impedance function, which fails to consider road node impedance. Conversely, the travel time calculated using the enhanced road impedance function model proposed by Wang exceeds the actual values. Notably, the results obtained from the novel road impedance function model developed in this study closely align with the actual driving time, surpassing the performance of other road impedance functions.

In the following sections, the actual travel time  $T$  under road impedance conditions will be used as the actual transport time of the vehicle.

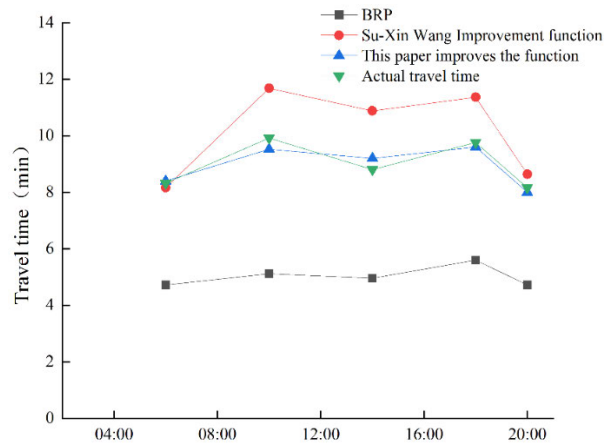


**FIGURE 3.** Comparison of travel times.

**IV. PROBLEM FORMULATION**

**A. PROBLEM DESCRIPTION**

The conundrum of optimizing the green logistics charging and switching path while taking into account the influence of road impedance is delineated as follows: A singular distribution center and an ample fleet of electric vehicles are at hand for distribution purposes. The geographic positioning of each customer point in relation to the charging station is known, as are the service time, time window, demand, and customer point location. Notably, the vehicle’s point of origin must be the distribution center. Furthermore, certain assumptions are upheld: firstly, all electric vehicles adhere to the same specifications, and both load and distance traveled must not exceed the vehicle’s maximum capacity. Secondly,

in addition to the power constraint, the distribution process must also adhere to the time window constraint. Thirdly, in instances where an electric vehicle lacks sufficient power to meet the distribution requisites, the vehicle must journey to the nearest charging station for recharging and replacement, under the condition that the station is fully charged. Lastly, the travel time of the vehicle during the transport process is calculated in accordance with the enhanced urban road impedance function model from the previous section. This mathematical model for electric vehicle logistics path optimization aims to minimize fixed costs, drive costs, electrical energy consumption costs, and charging and replacement costs.

## B. BATTERY DEGRADATION ANALYSIS

Electric vehicles rely on power exchange and fast or slow charging to replenish their electric energy. In logistics city distribution, time efficiency is crucial. Hence, we separately consider the charging and switching costs for fast charging and power exchange modes. Electric vehicles handle distribution tasks, returning to the distribution center for slow charging and discharging management. While generating profits, the battery incurs wear and tear costs accordingly.

The actual battery life is influenced by several factors, including the charging rate, state of charge, ambient temperature, and depth of discharge [35]. The effects of ambient temperature and depth of discharge are the primary considerations when employing Vehicle-to-Grid (V2G) technology for charging and discharging. In the case of lithium-ion batteries, the main principle behind battery loss is attributed to chemical reactions that take place within the battery, resulting in the formation of an oxide film on the electrode surface. Consequently, this leads to an increase in the internal resistance of the battery. Moreover, the ambient temperature directly impacts the rate of these chemical reactions occurring inside the battery, which typically follows the Arrhenius formula [35]

$$\mu = Ae^{-\frac{E}{kT}} \quad (12)$$

where  $\mu$  is the reaction rate;  $A$  is the Arrhenius constant in the same units as  $\mu$ ;  $E$  is the activation energy, a temperature-independent constant;  $k$  is the Boltzmann constant;  $T$  represents the absolute temperature,  $K$ .

Assuming the same time for each charge and discharge cycle, denoted by  $\Delta t$ , Then the increase in the internal resistance of the battery after a single cycle is obtained according to the Arrhenius formula.

$$\Delta r = r_0 Ae^{-\frac{E}{kT}} \Delta t \quad (13)$$

where  $r_0$  is the increment of resistance value per unit time, The unit is  $\Omega$ .

According to the test standard of lithium-ion battery cycle life, Combining with equation (2), the increase in internal resistance of a lithium-ion battery over its full life cycle can

be obtained as follows.

$$r_N = L_N r_0 A e^{-\frac{E}{kT_N} \Delta t} \quad (14)$$

The subscript  $N$  is the quasi-side value under standard conditions. It is known that at any temperature,  $T$ . The actual cycle life of the lithium-ion battery is

$$L = \frac{r_N}{\mu} = e^{\frac{E}{k} \left( \frac{1}{T} - \frac{1}{T_N} \right)} L_N \quad (15)$$

where  $e^{\frac{E}{k} \left( \frac{1}{T} - \frac{1}{T_N} \right)}$  is the temperature correction factor for the cycle life of the lithium-ion battery at temperature  $T$ , denoted as  $\omega$ .

The lifetime of Li-ion batteries is also dependent on the depth of discharge (DOD) during each charge and discharge cycle. The cycle life is shorter with a deeper depth of discharge [36], [37]. The battery life test value is measured at a 100% depth of discharge, implying that the actual battery life exceeds the nominal value under the same ambient temperature conditions. Additionally, an exponential relationship exists between the actual cycle life and the depth of discharge [38].

$$L = L_N D^{-0.795} \quad (16)$$

where:  $D$  represents the depth of discharge, expressed as a percentage;  $L_N$  represents the cycle life of the Li-ion battery under standard conditions ( $D = 1$ ).

Therefore, -0.795 can be defined as the depth-of-discharge correction factor for the cycle life of lithium-ion batteries at any depth of discharge ( $D$ ), denoted as  $\varphi$ .

## C. SYMBOLS AND DECISION VARIABLES

$M = \{1, 2, \dots, m\}$  is the set of the number of EVs used.  $N = \{0, 1, 2, \dots, n\}$  is the set of distribution centers and customer points.  $W = \{n, n + 1, \dots, n + m\}$  is the set of  $m$  charging stations.  $q_i$  is the demand of customer  $i$ .  $P_1$  is the fixed cost per unit of EV,  $P_2$  is the transportation cost per unit of time of EV,  $P_3$  is the price per unit of electricity consumption,  $P_4$  is the price per unit of time of fast charging electricity, and  $P_5$  is the cost of single exchange of electricity.  $Q, D$  denotes the maximum load and maximum distance of electric vehicle respectively.  $a_{ik}, [B_i, E_i]$  denotes the time of arrival of vehicle  $k$  at node  $i$ , and the time window of node  $i$ , respectively.  $E_0$  is the expected minimum charge during the driving of the electric vehicle.  $x_{ij}^k$  denotes the 0 – 1 variable,  $x_{ij}^k = 1$  when electric vehicle  $k$  is transported in section  $i, j$ , otherwise  $x_{ij}^k = 0$ .  $y_j^k$  denotes the 0 – 1 variable, if the electric vehicle  $k$  delivers for customer point  $j$ ,  $y_j^k = 1$ , otherwise  $y_j^k = 0$ .  $z_i^k$  denotes the 0 – 1 variable,  $z_i^k = 1$  when EV  $k$  is charging and exchanging at  $i$  charging station, otherwise  $z_i^k = 0$ .

A mathematical model of EV path optimization with a minimum total cost is constructed by considering charging and discharging cases. The cost is composed of fixed costs,

transportation costs, energy costs, charging and switching costs, slow charging and discharging costs, and battery wear and tear costs.

**D. MODEL BUILDING**

**1) FIXED COSTS AND TRANSPORTATION COSTS**

$$C_1 = K \times P_1 + P_2 \sum_{k=1}^m \sum_{i=0}^n \sum_{j=0}^n t_{ijk} x_{ij}^k \quad (17)$$

where  $K$  is the number of vehicles used,  $m$  is the number of vehicles available ( $k = 1, 2, \dots, m$ ), and  $t_{ijk}$  is the travel time of an electric vehicle in section  $i, j$ .

**2) TRANSPORTATION COSTS**

The energy consumption of electric vehicles is related to the load, speed, and transport time. In a time-varying road network environment. The power consumption of a vehicle traveling on road section  $[i, j]$  is

$$E_{ijk} = \sum_t^n P(Q_{ik}, v_{ijk}^t) * t_{ijk} \quad (18)$$

$$P(Q_k, v) = \frac{(Q_0 + Q_k) \cdot g \cdot f \cdot v + \frac{C_d \cdot A \cdot v^3}{21.15}}{3600\eta} \quad (19)$$

Therefore, the energy cost of electric vehicles is

$$C_2 = P_3 \sum_{k=1}^m \sum_{i=0}^n \sum_{j=1}^n x_{ij}^k t_{ijk} E_{ijk} \quad (20)$$

where  $P(Q_k, v)$  is the operating power,  $g$  is the acceleration of gravity,  $A, C_d, f$  is the wind-blown area of the electric vehicle, the air resistance coefficient and the friction resistance coefficient of the car,  $\eta$  is the mechanical transmission efficiency of the system, and  $Q_0, Q_k$  is the no-load and current load of the electric vehicle, respectively.

**3) FAST CHARGING OR POWER EXCHANGE COST**

When the remaining power of the electric vehicle is not enough to complete the distribution requirements to the next service point, it needs to go to the nearest charging station for quick charging. Charging costs are related to charging time. Charging time is  $t_{ik}^c = \frac{E_{\max} - E_{ik}}{r_c} z_i^k$ , charging costs is

$$C_{31} = P_4 \sum_{k=1}^m \sum_{i=0}^w t_{ik}^c \cdot z_i^k \quad (21)$$

where  $E_{\max}$  is the maximum battery capacity of the EV,  $E_{ik}$  is the power left in the EV at the charging station  $i$ , and  $r_c$  is the charging efficiency of the charging station.

The cost of power change is different from the charging method. The cost of the electric logistics vehicle is related to the number of times the electricity is changed. The cost of power change is

$$C_{32} = P_5 \sum_{k=1}^m \sum_{i=0}^w z_i^k \quad (22)$$

**4) SLOW CHARGING AND DISCHARGING COSTS AND BATTERY WEAR AND TEAR COSTS**

Electric vehicles return to the distribution center after completing the distribution task. They can be charged and discharged at the distribution center at a slow rate according to the time-sharing tariff to obtain certain benefits. The cost of charging and discharging is

$$C_4 = \left( a \sum_{T_0}^{T_1} P_c W_c - b \sum_{T_0}^{T_1} P_d W_d \right) (T_1 - T_0) \quad (23)$$

where  $P_c$  and  $P_b$  denotes the charging tariff and discharging tariff respectively,  $W_c$  and  $W_b$  denotes the charging power and discharging power respectively.  $a$  and  $b$  denotes the charging and discharging parameters respectively. When charging,  $a$  is 1 and  $b$  is 0. When discharging,  $a$  is 0 and  $b$  is 1.  $T_0$  and  $T_1$  denotes the start time and end time of charging and discharging respectively.

$$C_6 = \frac{P_b}{\omega\phi L_N E_{\max}} \quad (24)$$

In summary, the total cost of distribution and charging/discharging in the fast-charging mode of electric vehicles is modeled as follows

$$C = K \times P_1 + P_2 \sum_{k=1}^m \sum_{i=0}^n \sum_{j=0}^n t_{ijk} x_{ij}^k + P_3 \sum_{k=1}^m \sum_{i=0}^n \sum_{j=1}^n x_{ij}^k t_{ijk} E_{ijk} + P_4 \sum_{k=1}^m \sum_{i=0}^w t_{ik}^c \cdot z_i^k + \left( a \sum_{T_0}^{T_1} P_c W_c - b \sum_{T_0}^{T_1} P_d W_d \right) (T_1 - T_0) + \frac{P_b}{\omega\phi L_N E_{\max}} \quad (25)$$

The constraints are as follows

$$\sum_{k=1}^m \sum_{i=1}^n x_{ij}^k \leq m, i = 0 \quad (26)$$

$$\sum_{k=1}^m \sum_{j=1}^n x_{ij}^k = \sum_{k=1}^m \sum_{j=1}^n x_{ji}^k, i = 0, k = 1, 2, \dots, m \quad (27)$$

$$\sum_{k=1}^m y_i^k = 1, i = 1, 2, \dots, n \quad (28)$$

$$\sum_{i=1}^n q_i y_i^k \leq Q, i \neq j, k = 1, 2, \dots, m \quad (29)$$

$$\sum_{i=0}^n \sum_{j=0}^n d_{ij} x_{ij}^k \leq D, i \neq j, k = 1, 2, \dots, m \quad (30)$$

$$a_{ik} + t_{ik} \geq B_i \quad (31)$$

$$a_{ik} + t_{ik} \leq E_i \quad (32)$$

$$\sum_{k=1}^m \sum_{i=0}^w E_{ik}^a (1 - z_i^k) + E_{\max}$$

$$= \sum_{k=1}^m \sum_{i=0}^w E_{ik}^l \quad (33)$$

$$E_0 \leq E_{ik}^a \leq E_{\max} \quad (34)$$

(26) states that the number of electric vehicles used for distribution should be equal to or greater than the number of distribution routes. (27) specifies that the starting point for each distribution vehicle must be a distribution center to complete its assigned distribution mission. (28) indicates that each demand point can only be served by one electric vehicle, and just once. (29) ensures that the total demand of customer points in each distribution route must not exceed the maximum carrying capacity of electric vehicles. (30) mandates that the total distribution distance of each distribution path should not exceed the electric vehicle’s maximum distribution distance. (31) and (32) represent the time window constraints. (33) requires the electric vehicle to depart after recharging at the charging station. (34) refers to the power constraint for each electric vehicle at every customer point.

The total cost model of distribution and charging and discharging in the electric vehicle switching mode is

$$C' = K \times P_1 + P_2 \sum_{k=1}^m \sum_{i=0}^n \sum_{j=0}^n t_{ijk} x_{ij}^k + P_3 \sum_{k=1}^m \sum_{i=0}^n \sum_{j=1}^n x_{ij}^k t_{ijk} E_{ijk} + P_5 \sum_{k=1}^m \sum_{i=0}^w z_i^k + \left( a \sum_{T_0}^{T_1} P_c W_c - b \sum_{T_0}^{T_1} P_d W_d \right) (T_1 - T_0) \quad (35)$$

The constraints are as above.

### V. ALGORITHM RESEARCH

Addressing Charge/Transfer Electric Vehicle Routing Problem Models while accounting for road impedance leads to a significant computational challenge. When employing an exact algorithm, the search process is characterized by a sluggish pace. Therefore, heuristic algorithms are commonly favored for tackling such NP-hard conundrums. Notably, the genetic algorithm emerges as an efficient parallel search technique, well-suited for resolving global optimization predicaments. The distinct procedural steps of the genetic algorithm in addressing the Electric Vehicle Routing Problem are delineated as follows.

Step 1: Encoding and Decoding. When addressing the Electric Vehicle Routing Problem, the selection of paths necessitates the consideration of both the load impact and the imperative to visit charging stations for recharging when the electric vehicle’s power reserve is low. To articulate the sequence of customer visitations within the instance, customers are encoded using natural numbers, where each customer is denoted by a unique number, 1, 2, ..., n. Meanwhile, the distribution center is assigned the number 0. In scenarios featuring m charging stations, the charging station numbers are allocated as n+1, ..., n+m. The initial

customer nodes are orderly arranged in an integer sequence, with the distribution center 0 interposed among the customer points in accordance with constraints such as the vehicle’s maximum load and the demand at each node. Furthermore, contingent upon the remaining power level of the electric vehicle, a determination is made regarding the necessity to journey to the nearest charging station for recharging. Should recharging be deemed necessary, the corresponding charging station number is subsequently inserted after the customer point number.

Consider, for instance, the sequential arrangement of integers (6,2,5,4,3,1,7,10,9,8) representing the order of customer points. Following the insertion of the distribution center in compliance with load and time window constraints, the resulting arrangement is (0,6,2,5,0,4,3,1,7,0,10,9,8,0). Subsequently, when the electric vehicle’s power reserve is low, the charging station is inserted, leading to the arrangement(0,6,2,11,5,0,4,12,3,1,7,0,10,9,8,0).The process of decoding serves as the inverse of encoding, whereby the path following the decoding of this chromosome unfolds as follows:

- Path 1: 0,6,2,11,5,0
- Path 2: 0,4,12,3,1,7,0
- Path 3: 0,10,9,8,0

This configuration signifies the utilization of three electric vehicles for delivery, with a total of two recharging stops en route.

Step 3: The fitness function is determined. The EVRP model, designed for both deterministic conditions and robust optimization, endeavors to minimize the total cost. As the chromosome fitness value increases, so does the likelihood of inheritance in the subsequent generation. Hence, the fitness function is defined as the inverse of the objective function.

Step 4: Selection. Initially, the elite retention strategy was employed for selection, wherein the fitness values are sorted in descending order. The top 5% of chromosomes are preserved as elite for the subsequent generation, while the remaining 95% are chosen using the roulette wheel selection method. A subset of high-fitness chromosomes is then earmarked for crossover and mutation to constitute the succeeding generation’s population.

Step 5: Crossover. In the process of chromosome coding in the EVRP problem, the insertion of the charging station number will occur, and crossover and mutation will be performed. The original insertion position of the charging station will be destroyed, and many inferior solutions will appear in the offspring. Therefore, the inserted genes should be removed before the crossover and mutation operations. The crossover operation selects genes that are not duplicated on the parent chromosome and puts them into the offspring sequentially. For example, the parents P1 (1,2,3,4,5,6,7) and P2 (6,4,2,3,7,1,5), after crossover, the offspring O1 (1,6,2,4,3,5,7,1) and O2 (6,1,4,2,3,7,5).

Step 6: Mutation. Genetic variation manifests consistently during genetic manipulation to forestall premature local convergence and uphold chromosome diversity. Mutating



**TABLE 1.** Time-sharing tariff.

Types	Time period	Charge Price (yuan/kwh)	Discharge price (yuan/kwh)
Peak hours	10:00-20:00	1.28	0.9
Non-peak hours	00:00-10:00 20:00-24:00	0.35	0.20

chromosomes is imperative in this regard. During the mutation operation, a subset of gene positions on the parent chromosome are randomly chosen and subsequently reorganized, while the remainder of the positions remain unaltered.

Step 7: The evolutionary reversal operation serves to enhance solution quality and expedite local convergence. This operation is executed on chromosomes that have already undergone selection and crossover mutation. During the reversal operation, two random integers are generated to determine the chromosome positions, and the sequence between these positions is reversed to yield a new chromosome. For instance, given parent P1 (1,2,3,4,5,6,7), random integers 3 and 6 produce offspring O1 (1,2,6,5,4,3,7) after reversal. Importantly, only reversals resulting in heightened fitness values are considered valid.

The algorithm is designed to terminate automatically after 500 iterations, ensuring that the output result is obtained within this specified number of computational cycles.

## VI. EXAMPLE ANALYSIS

### A. DATA AND PARAMETER SETTINGS

The experimental data is retrieved from the figshare database (<https://doi.org/10.6084/m9.figshare.10288326>). The simulation data selected for analysis is the R-2-C-30 example, comprising 30 customer points and 2 charging stations. Customer nodes are represented by numbers 1 to 30, while the distribution center is denoted as 0, and the charging stations are represented by 31 and 32. The known information for each customer point includes their demand, service time, and time window.

Electric vehicles perform distribution tasks and subsequently return to the distribution center, where they interface with the grid via batteries. They have the capability to both draw electricity from and supply electricity to the grid, enabling the sale of surplus electricity to the open market with the objective of realizing profitable returns in accordance with time-of-use tariffs. This decision-making process leverages time-of-use tariff data sourced from pertinent literature [12], thereby optimizing charging and discharging activities. The temporal structure is delineated into peak and off-peak periods, which are delineated as time-of-day tariffs in Table 1. Upon completing their distribution tasks, electric vehicles regroup at the distribution center to connect to the grid via batteries. Here, they engage in either procuring

electricity from or feeding electricity into the grid, with the ultimate goal of capitalizing on the time-of-use tariffs to yield a profit. These decisions are informed by the time-of-use tariff data gleaned from the pertinent literature [39].

The problem was tackled using a genetic algorithm on a computer processor operating at a frequency of 2.20 GHz and equipped with 4 GB of memory, while making use of MATLAB (R2018b). The specific parameters employed in this configuration are detailed in Table 2.

### B. ANALYSIS OF THE RESULTS

In order to evaluate the effectiveness of considering the impact of dozos impedance in EVRP and the proposed path planning and charging/discharging management models, four different scenarios were created for comparative analysis. Scenarios 1 and 2 entail the use of power switching and fast charging methods, respectively, to minimise costs through path optimisation of distribution routes. Scenarios 3 and 4 are derived from the logistics distribution of Scenarios 1 and 2, and the influence of road impedance is considered in the transport time, which is calculated by applying the improved road impedance model in the above section. According to the relevant information, the headway distance is set to 2 m, and the average length of motor vehicles is set to 6 m. Through real-time road development tools such as Baidu Maps, it is determined that the theoretical blockage density of a single lane,  $K_j$ , is about 125 vehicles/km. By analysing the nature of the road between individual customer points, the average traffic density  $K$  value of different road attributes is derived. It is worth noting that the fast charging approach takes into account the cost of battery depletion. Using a genetic algorithm, we solved the R-2-C-30 instances for the four cases. Figures 4 to 7 show the optimisation maps for the EV distribution paths.

The depicted figure illustrates a notable reduction in the frequency of intersections among EV distribution routes in Cases 2 and 4 when compared to Cases 1 and 3. A higher intersection count corresponds to elongated total logistics and distribution paths, consequently leading to escalated logistics and distribution expenses as well as extended charging durations. Specifically, the utilization of fast charging during transportation in two models results in prolonged charging periods in contrast to the model employing power switching. This disparity in charging duration is attributed

TABLE 2. Model parameter values.

Parameters	Parameter Value	Parameters	Parameter Value
$P_1$	100 yuan/veh	$Q_0$	2t
$P_2$	50yuan/h	$\mathcal{G}$	$9.81 m / s^2$
$P_3$	0.5 yuan/kwh	$f$	0.015
$P_4$	1yuan/min	$C_d$	0.6
$P_5$	100yuan/time	$P_b$	60000yuan
$L_N$	800time	$E_{max}$	100kw.h
$Q$	100kg	$v$	40km/h
$\hat{\partial}$	0.01	$\eta$	1.46
$W_c$	9kw	$W_d$	6kw
$A$	$6 m^2$	$r_c$	2 kw/h

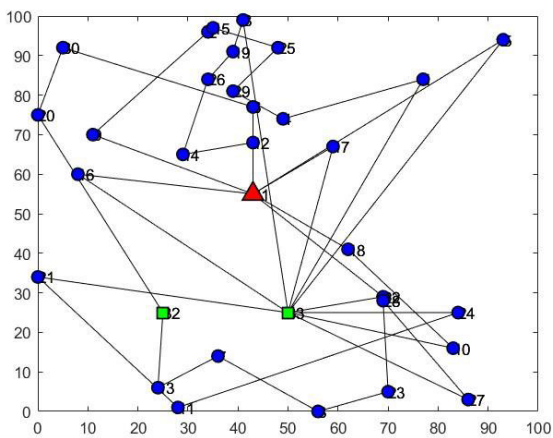


FIGURE 4. Scenario 1.

to the intricacy and associated costs of fast charging relative to switching. Consequently, an elevated number of path intersections contributes to amplified costs and temporal requirements, culminating in augmented total distribution expenses.

The experimental findings furnish insights into the frequency and duration of charging and discharging activities across four distinct scenarios. Notably, Scenario 4 exhibits a heightened charge change frequency and duration in comparison to Scenario 2. Similarly, Scenario 3 manifests a greater frequency and prolonged aggregate charging duration than Scenario 1. The charging durations (in hours) for Scenario 1 are recorded as 1.12, 1.14, 0.81, 0.43, 0.91, and 1.05, while those for Scenario 3 are 1.34, 0.61, 1.05, 0.79, and 0.36. This variance primarily stems from the incorporation of road impedance effects in Scenarios 4 and 3, whereas

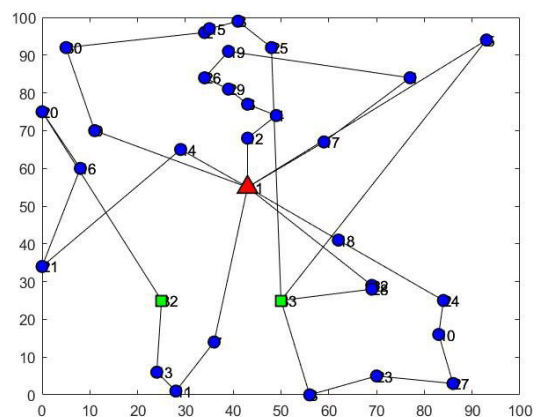


FIGURE 5. Scenario 2.

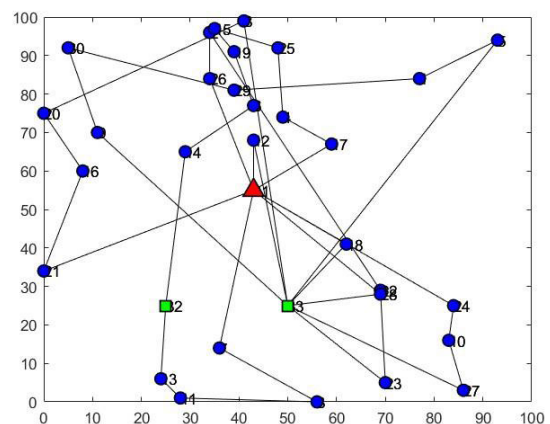


FIGURE 6. Scenario 3.

Scenarios 1 and 2 are characterized by ideal travel velocities and durations, translating to reduced transportation durations

TABLE 3. Optimal vehicle routing.

Vehicle number	Distribution route	
	Scenario 1	Scenario 3
1	0 → 12 → 14 → 26 → 19 → 8 → 32 → 10 → 18 → 0	0 → 24 → 10 → 27 → 32 → 9 → 30 → 29 → 1 → 5 → 32 → 12 → 0
2	0 → 6 → 30 → 20 → 31 → 13 → 7 → 3 → 23 → 28 → 27 → 32 → 17 → 0	0 → 17 → 4 → 25 → 15 → 19 → 6 → 14 → 31 → 13 → 11 → 3 → 7 → 0
3	0 → 9 → 2 → 15 → 25 → 29 → 4 → 1 → 32 → 21 → 11 → 24 → 32 → 16 → 0	0 → 26 → 2 → 22 → 23 → 32 → 18 → 0
4	0 → 5 → 32 → 22 → 0	0 → 21 → 16 → 20 → 8 → 32 → 28 → 0

TABLE 4. Optimal cost comparison.

COST	Scenario1	Scenario2	Scenario3	Scenario4
GC	400	400	400	400
YC	929.96	673.20	1138.15	808.14
NC	140.95	169.93	214.81	185.18
CC	209.74	0	290.16	0
HC	0	300	0	400
VC	-18	-61.2	-18	-61.2
DC	12.05	0	12.05	0
TC	1674.70	1481.94	2037.17	1732.12

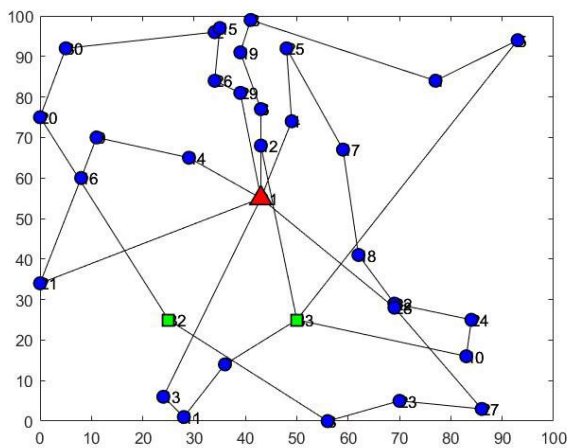


FIGURE 7. Scenario 4.

and energy consumption. Consequently, energy consumption is curtailed, and the frequency and duration of charging and switching activities are diminished. Hence, the integration of road impedance effects renders the transportation scenarios more pragmatic and augments the efficiency of the outcomes.

The specific optimized path outcomes for Scenario 1 and Scenario 3 are delineated in Table 3.

The experimental outcomes pertaining to each expense category are detailed in Table 4. In this context, GC denotes the fixed costs, YC signifies the transportation expenses, NC represents the energy outlays, CC encapsulates the charging costs, HC embodies the fluctuating electricity expenses, VC denotes the costs associated with slow charging and discharging, DC encapsulates the battery depletion charges, and TC encompasses the aggregate costs, all of which are quantified in yuan.

Evidently, as illustrated in Table 3,

(1) A comparative analysis of the expenditure associated with the two paradigms in Scenario 1 and Scenario 3 reveals that the latter exhibits elevated transportation, energy, and charging costs in contrast to the former. This disparity stems from the fact that the derived transport duration, calculated employing the road impedance function, surpasses the unimpeded transport time in Scenario 1. Furthermore, all four costing methodologies of the focal model in this investigation are intertwined with the transport duration. The cost of slow charging and discharging back to the distribution center is

**TABLE 5. Ambient Temperature Sensitivity Analysis.**

T	30°C	20°C	10°C	1°C
<b>DC (70%)</b>	<b>12.14</b>	<b>12.01</b>	<b>11.44</b>	<b>4.53</b>

**TABLE 6. Discharge depth sensitivity analysis.**

D	100%	70%	50%	30%
<b>DC (20°C)</b>	<b>16</b>	<b>12.12</b>	<b>9.32</b>	<b>6.45</b>

unaffected by the battery degradation in relation to the transport time; hence, minimal alteration is observed between the two scenarios. The disparity in total cost between Scenario 1 and Scenario 3 amounts to 21.64%, underscoring the substantial influence of accounting for road impedance in EV logistics transport on the overall expenditure. Accordingly, it is imperative to factor in the influence of road impedance on transport, thereby aligning transport duration with real-world constraints.

(2) As above, a comparison of the costs of the two models from Scenario 2 and Scenario 4 shows that Scenario 4 has higher transport costs, energy costs, and power change costs compared to Scenario 2. Scenario 4 has one more power change. Therefore, the cost of power change is higher. Other cost reasons are similar to the comparison of scenarios under fast charging. The percentage difference between the total cost of Scenario 2 and Scenario 4 is 16.88%, which indicates that whether or not to consider the road impedance situation has a relatively small impact on the total cost of distribution in the power exchange scenario. This is also related to the fact that power exchange is more efficient than fast charging.

(3) The costs in Cases 2 and 4 are \$43.2 lower than those incurred in slow charging and discharging in Cases 1 and 3. This divergence primarily stems from the replenishment of power during the distribution process facilitated by the switching method, obviating the necessity to factor in battery depletion resulting from charging and discharging. In contrast, charging entails expenses associated with battery depletion, which are predominantly influenced by the depth of discharge. Consequently, the superiority of employing slow charging and discharging at the distribution center becomes more conspicuous in the switching mode, eliminating concerns about battery depletion.

(4) The optimal solution for all four scenarios entails the utilization of four electric vehicles for delivery. Among these scenarios, the total delivery cost is lower in Scenario 2 than

in Scenario 1. This discrepancy is primarily ascribed to the extended duration spent on fast charging during transportation and the imperative for multiple charging occurrences stemming from varying degrees of battery aging. Within the model, transportation costs are predominantly influenced by the duration of transport, resulting in escalated overall transportation expenses. Furthermore, the necessity for multiple trips to the charging station for recharging incurs additional energy costs. Although the cost of a single switch surpasses the average cost of a single switch, the disparity in switching costs to accomplish the final distribution task is not substantial owing to the quantity of switches involved. Consequently, the choice of power exchange mode for logistics and distribution in Case 1 proves to be more economically efficient.

### C. BATTERY LOSS SENSITIVITY ANALYSIS

The efficacy of electric vehicle batteries during discharge to the grid is chiefly influenced by ambient temperature and depth of discharge. The empirical results are delineated in Table 5 and Table 6, with the effects of ambient temperature and depth of discharge on battery degradation illustrated in Figures 8 and 9.

From the graph above, it is evident that the depth of discharge remains constant. With the rise in ambient temperature, the battery loss cost also increases. The trend of the curve indicates that higher temperatures lead to a smaller magnitude of increased cost loss. This is mainly due to the fact that the higher the temperature, the lower the temperature correction factor  $\omega = e^{\frac{k}{T}(\frac{1}{T} - \frac{1}{T_N})}$  and the smaller the magnitude of the curve. Similarly, at a constant ambient temperature of 20 degrees Celsius The deeper the discharge depth is, the lower the correction factor  $\sigma = D^{-0.795}$  is, and the magnitude of the reduction is not significant. Consequently, the greater the depth of discharge, the higher the cost of battery deterioration.



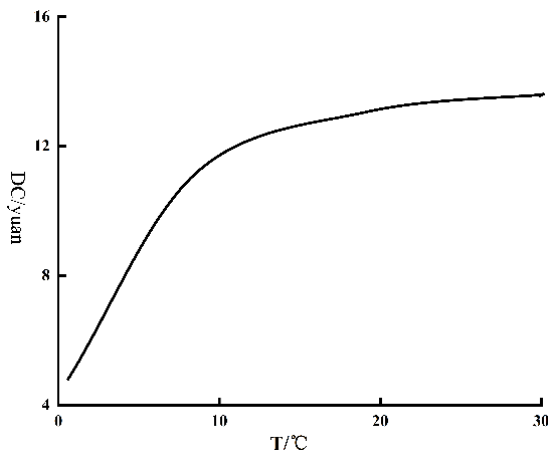


FIGURE 8. Trend of temperature on battery.

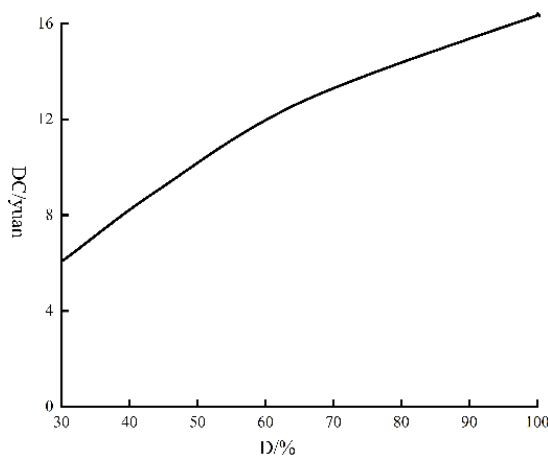


FIGURE 9. Trend of depth of discharge on battery loss.

While prolonged charging and discharging may indeed impact battery longevity, tailored charging and discharging tactics can be tailored to individual tariff periods in order to meet specific revenue objectives. This approach serves to mitigate base loads and redistribute peak loads during periods of heightened power consumption, thereby markedly alleviating grid load fluctuations. The simulation data expounded in this paper pertains to a singular investigation within the small-scale distribution domain of the logistics sector. Nevertheless, the charge/discharge management model explicated in this paper possesses the potential for extrapolation to large-scale logistics distribution services, thereby optimizing power efficiency and substantially diminishing peak-to-valley load differentials.

## VII. CONCLUSION

In recent years, with the acceleration of urbanisation and the enhancement of environmental awareness, the development of green logistics systems has become a research priority in the field of urban logistics. In this framework, electric vehicles, as a model of clean energy, have received widespread

attention. In this paper, road impedance is applied to the charging and path optimisation problems of green logistics vehicles, which is of great significance for improving logistics efficiency, reducing transport costs and improving urban environment. The results of this paper are as follows: (1) In comparison with the fast charging mode, the switching mode, complemented by distribution path planning, diminishes path complexity and the overall cost of concurrent deliveries. (2) The power switching mode of electric vehicles presents lower distribution costs under specific conditions, particularly in locales with high urban impediments. (3) The integration of a road impedance model into green logistics vehicle charging, switching, and path optimization can effectively enhance distribution efficiency, reduce transportation costs, and exert a positive influence on urban environments. (4) The results from the refined genetic algorithm evince that the green logistics vehicle charging and path optimization model, accounting for road impedance, can more accurately mirror the actual conditions of urban thoroughfares and improve the feasibility and precision of path planning. (5) The costs stemming from electric vehicle battery degradation increase with declining ambient temperatures and uniformly escalate with rising discharge depths.

In the future based on this research the following directions can be extended: firstly, enhancing the charging and path optimisation models for green logistics vehicles to enable more complex and tailored path planning to suit different attributes of different cities and road networks. Secondly, with the integration of real-time traffic data and the distribution of charging infrastructure, exploring charging, switching and path optimisation for green logistics vehicles using big data and artificial intelligence techniques will enhance the intelligence and immediacy of planning and decision-making. Finally, charging and switching strategies for various types of electric vehicles (including pure electric vehicles and plug-in hybrids) under urban impedance conditions are explored and comparatively assessed in terms of distribution efficiency and cost with conventional fuel vehicles.

## REFERENCES

- [1] N. Batarliene and D. Bazaras, "Solutions to the problem of freight transport flows in urban logistics," *Appl. Sci.*, vol. 13, no. 7, p. 4214, Mar. 2023.
- [2] A. Nikseresht, D. Golmohammadi, and M. Zandieh, "Sustainable green logistics and remanufacturing: A bibliometric analysis and future research directions," *Int. J. Logistics Manag.*, vol. 14, pp. 1–16, Jul. 2023.
- [3] S. S. Grzesiak and A. Sulich, "Electromobility: Logistics and business ecosystem perspectives review," *Energies*, vol. 16, no. 21, p. 7249, Oct. 2023.
- [4] L. M. Oliveri, D. D'Urso, N. Trapani, and F. Chiacchio, "Electrifying green logistics: A comparative life cycle assessment of electric and internal combustion engine vehicles," *Energies*, vol. 16, no. 23, p. 7688, Nov. 2023.
- [5] Q. Guo, N. Wang, B. Su, and M. Zhang, "Bi-objective vehicle routing for muck transportation in urban road networks," *IEEE Access*, vol. 8, pp. 114219–114227, 2020.
- [6] N. Huang, L. Hu, R. Wang, G. Cai, Y. Guo, and X. Zhao, "Multi-objective optimal scheduling of distribution network with electric vehicle charging load considering time-varying road impedance," *J. Electr. Eng. Technol.*, vol. 18, no. 4, pp. 2667–2681, Jan. 2023.
- [7] W. Wang, J.-C. Chen, and Y. J. Wu, "The prediction of free-way traffic conditions for logistics systems," *IEEE Access*, vol. 7, pp. 138056–138061, 2019.

- [8] J. Xu, D. Hu, and Y. Liang, "Optimization of distribution route of fresh products considering carbon emissions and traffic congestion," in *Proc. CICTP*, 2020, pp. 4433–4444.
- [9] T. Zhang, J. Xu, S. Cong, C. Qu, and W. Zhao, "A hybrid method of traffic congestion prediction and control," *IEEE Access*, vol. 11, pp. 36471–36491, 2023.
- [10] M. B. Younes and A. Boukerche, "An efficient dynamic traffic light scheduling algorithm considering emergency vehicles for intelligent transportation systems," *Wireless Netw.*, vol. 24, no. 7, pp. 2451–2463, Oct. 2018.
- [11] J. Chen, W. Liao, and C. Yu, "Route optimization for cold chain logistics of front warehouses based on traffic congestion and carbon emission," *Comput. Ind. Eng.*, vol. 161, Nov. 2021, Art. no. 107663.
- [12] X. Guo, W. Zhang, and B. Liu, "Low-carbon routing for cold-chain logistics considering the time-dependent effects of traffic congestion," *Transp. Res. D, Transp. Environ.*, vol. 113, Dec. 2022, Art. no. 103502.
- [13] A. B. Zhang, Y. Zhang, and Y. Q. Liu, "Low-carbon cold-chain logistics path optimization problem considering the influence of road impedance," *IEEE Access*, vol. 11, pp. 124055–124067, 2023.
- [14] Z. Zhao, X. Li, and X. Zhou, "Distribution route optimization for electric vehicles in urban cold chain logistics for fresh products under time-varying traffic conditions," *Math. Problems Eng.*, vol. 2020, pp. 1–17, Oct. 2020.
- [15] L. Y. Hou, C. Wang, and J. Yan, "Electric vehicle charging scheduling in green logistics: Challenges, approaches and opportunities," 2021, *arXiv:2103.07635*.
- [16] M. Haghani, F. Sprei, K. Kazemzadeh, Z. Shahhoseini, and J. Aghaei, "Trends in electric vehicles research," *Transp. Res. D, Transp. Environ.*, vol. 123, Oct. 2023, Art. no. 103881.
- [17] K. Li and L. Wang, "Optimal electric vehicle subsidy and pricing decisions with consideration of EV anxiety and EV preference in green and non-green consumers," *Transp. Res. E, Logistics Transp. Rev.*, vol. 170, Feb. 2023, Art. no. 103010.
- [18] S. Imre, D. Çelebi, and U. Asan, "Estimating potential adoption rate of electric vehicles in urban logistics," *Transp. Planning Technol.*, vol. 13, pp. 1–30, Nov. 2023.
- [19] L. Timilsina, P. R. Badr, P. H. Hoang, G. Ozkan, B. Papari, and C. S. Edrington, "Battery degradation in electric and hybrid electric vehicles: A survey study," *IEEE Access*, vol. 11, pp. 42431–42462, 2023.
- [20] H. Qiang, R. Ou, Y. Hu, Z. Wu, and X. Zhang, "Path planning of an electric vehicle for logistics distribution considering carbon emissions and green power trading," *Sustainability*, vol. 15, no. 22, p. 16045, Nov. 2023.
- [21] B. Zhou and Z. Zhao, "Multi-objective optimization of electric vehicle routing problem with battery swap and mixed time windows," *Neural Comput. Appl.*, vol. 34, no. 10, pp. 7325–7348, Feb. 2022.
- [22] Z. Shangquan and D. Qi, "Charging station planning of electric vehicle in battery swapping scene," *J. Phys., Conf.*, vol. 2354, no. 1, Oct. 2022, Art. no. 012004.
- [23] B. Zhao, H. Gui, H. Li, and J. Xue, "Cold chain logistics path optimization via improved multi-objective ant colony algorithm," *IEEE Access*, vol. 8, pp. 142977–142995, 2020.
- [24] L.-Y. Zhang, M.-L. Tseng, C.-H. Wang, C. Xiao, and T. Fei, "Low-carbon cold chain logistics using ribonucleic acid-ant colony optimization algorithm," *J. Cleaner Prod.*, vol. 233, pp. 169–180, Oct. 2019.
- [25] G. Qin, F. Tao, and L. Li, "A vehicle routing optimization problem for cold chain logistics considering customer satisfaction and carbon emissions," *Int. J. Environ. Res. Public Health*, vol. 16, no. 4, p. 576, Feb. 2019.
- [26] X. Y. Ren, "Path optimization of cold chain distribution with multiple distribution centers considering carbon emissions," *Appl. Ecology Environ. Res.*, vol. 17, no. 4, pp. 9437–9453, 2019.
- [27] M.-X. Song, J.-Q. Li, Y.-Q. Han, Y.-Y. Han, L.-L. Liu, and Q. Sun, "Metaheuristics for solving the vehicle routing problem with the time windows and energy consumption in cold chain logistics," *Appl. Soft Comput.*, vol. 95, Oct. 2020, Art. no. 106561.
- [28] L. Zhu and D. Hu, "Study on the vehicle routing problem considering congestion and emission factors," *Int. J. Prod. Res.*, vol. 57, no. 19, pp. 6115–6129, Oct. 2019.
- [29] Z. Wang and P. Wen, "Optimization of a low-carbon two-echelon heterogeneous-fleet vehicle routing for cold chain logistics under mixed time window," *Sustainability*, vol. 12, no. 5, pp. 1967–1987, Mar. 2020.
- [30] J. Chen, P. Gui, T. Ding, S. Na, and Y. Zhou, "Optimization of transportation routing problem for fresh food by improved ant colony algorithm based on Tabu search," *Sustainability*, vol. 11, no. 23, pp. 6584–6604, Nov. 2019.
- [31] S. X. Wang, L. Z. Wang, L. Gao, X. G. Cui, and X. M. Chen, "Improvement study on BPR link performance function," *J. Wuhan Univ. Technol.*, vol. 33, no. 3, pp. 446–449, Jun. 2009.
- [32] B. Zhou, L. P. Zhi, and B. Li, "Improved BPR impedance function and its application in EMME," *J. Shanghai Maritime Univ.*, vol. 34, no. 4, pp. 67–70, Dec. 2013.
- [33] Y. Y. Pan, T. Yu, and J. X. Ma, "Improvement of urban road impedance function based on section impedance and node impedance," *J. Chongqing Jiaotong Univ., Natural Sci.*, vol. 36, no. 8, pp. 76–81, Aug. 2017.
- [34] R. Ma, X. Wang, and P. Zhou, "Research on optimization of fresh cold chain logistics distribution path considering road impedance," in *Proc. Int. Signal Process., Commun. Eng. Manag. Conf. (ISPCEM)*, Nov. 2020, pp. 185–192.
- [35] S. Han, S. Han, and H. Aki, "A practical battery wear model for electric vehicle charging applications," *Appl. Energy*, vol. 113, pp. 1100–1108, Jan. 2014.
- [36] T. Perger and H. Auer, "Energy efficient route planning for electric vehicles with special consideration of the topography and battery lifetime," *Energy Efficiency*, vol. 13, no. 8, pp. 1705–1726, Sep. 2020.
- [37] B. Xu, J. Shi, S. Li, H. Li, and Z. Wang, "Energy consumption and battery aging minimization using a Q-learning strategy for a battery/ultracapacitor electric vehicle," *Energy*, vol. 229, Aug. 2021, Art. no. 120705.
- [38] P. Li, X. Xia, and J. Guo, "A review of the life cycle carbon footprint of electric vehicle batteries," *Separat. Purification Technol.*, vol. 296, Sep. 2022, Art. no. 121389.
- [39] M. B. Rasheed, M. Awais, T. Alquthami, and I. Khan, "An optimal scheduling and distributed pricing mechanism for multi-region electric vehicle charging in smart grid," *IEEE Access*, vol. 8, pp. 40298–40312, 2020.



**LEI FU** received the master's degree in business administration from Northeastern University. She is currently an Associate Professor with the School of Science and Technology, Shenyang Polytechnic College. Her main research interest includes technology innovation management.



**YAN XU** received the degree in information management from Benedict University, USA. His main research interest includes the development and application of information technology.



**AOBEI ZHANG** received the degree from the School of Management, Shenyang University of Technology, where he is currently pursuing the Ph.D. degree in logistics engineering and management. His research interests include complex system decision-making and optimization, logistics path optimization, and intelligent optimization algorithms.